INFORMATICS JOURNALS

ISSN (Print) : 0013-466X
ISSN (Online) : xxxx-xxxx

The Journal of Electrochemical Society of India, Volume 75, Issue (2), April-June 2026; pp. 126-139

DOI: 10.18311/JESCI/2026/56331

Synergistic Role of Ceria and Titania in Enhancing the Microhardness and Corrosion Resistance of Electrodeposited Ni-Ceria-Titania Composite Coating

J. Ann Miriam[1], N. Balaji[1] and S. T. Aruna[1,2*]

[1]Surface Engineering Division, CSIR- National Aerospace Laboratories, Bengaluru - 560017, Karnataka, India
[2]Academy of Scientific and Innovative Research (AcSIR), Ghaziabad - 201002, Uttar Pradesh, India

Abstract

Electrodeposited composite coatings are of great importance due to their wide range of applications. Among them, electrodeposited Ni-composite coatings are widely studied for wear and corrosion resistance applications. The properties of the composite coatings can be tailored by the filler particles. In the literature, many filler particles like alumina, ceria, titania, zirconia, SiC, Si_3N_4, etc., have been explored as the distributive phases in the Ni composite coatings. In the present study, ceria-titania composite powder corresponding to 73 wt% TiO_2 and 27 wt% CeO_2 was used as the distributive phase in the Ni matrix to obtain Ni-TC coating. The effect of particle loading (25 and 100 g/L) on the particle incorporation and microhardness of the Ni composite coating has been studied. The best coating exhibited the highest Knoop hardness of 525 at 50 gF. The optimized Ni-TC coating exhibited improved corrosion resistance compared to plain Ni, Ni-TiO_2 and Ni-CeO_2 coatings reported in the literature. This study proves that titania-ceria composite powders are promising distributive phases for electrodeposited Ni composite coatings to improve the microhardness, corrosion and wear resistance. Further, the titania and ceria powders synergistically contribute to the coating properties.

Keywords: Composite, Corrosion, Electrodeposited, Microhardness, Nickel, Wear

1. Introduction

There is a great demand for composite coatings for a myriad of engineering applications in various sectors. It has been widely accepted that electrodeposition is one of the most important methods for developing nanocomposite coating as it is cheaper, does not require sophisticated equipment, high pressures and temperatures[1]. Electrodeposited nickel is an important functional coating that is used due to its ductility, higher hardness, excellent corrosion resistance and good wear resistance. However, to match the Ni coating properties to that of the conventional hard chrome coating, composite coatings have been explored. Since the properties of the composite coatings are dependent on the nature of the particles, various filler particles have been explored to tailor the properties of the Ni-composite coating[2-5]. The dispersed fillers enhance the mechanical, tribological and corrosion resistant properties of the composite coatings. The mechanical and wear resistant properties of the composite coatings are significantly enhanced as they act as physical barriers to dislocation movement and grain boundary sliding[1-5]. Based on the filler particles used, these Ni-composite coatings can find applications such as in (i) aerospace components, (ii) automotive engine parts, (iii) cutting and drilling tools, (iv) industrial components that undergo wear, (v) textile machinery, (vi) electrical contacts, (vii) anticorrosion coatings, (viii) agricultural machineries, (ix) medical devices, (x) self-cleaning and photocatalytic coatings, (xi) mining equipment, etc[2-5]. Ni-SiC is one of the

*Author for correspondence

*Email: aruna_reddy.nal@csir.res.in

important commercial coatings that is widely used in automotive industry for improving the wear resistance. In this direction, different micron and nanosized filler particles like alumina, ceria, diamond, SiC, Si_3N_4, titania, yttria doped ceria, Al_2O_3-TiO_2, pumice, oil filled microcapsules, cenosphere, mullite, $ZnAl_2O_4$, CNTs, graphene, zircon, pumice, etc have been explored[6-38].

With the increasing availability of nanoparticles, there is a growing interest in developing newer composite coatings. Amidst the renewed interest in composite coatings, titania is the most widely used material because of its good photocatalytic property. It is widely used in self-cleaning coatings, pigments, dye-sensitized solar cells, etc. It exists in three different phases: anatase, brookite and rutile. Titania nanoparticles have been used to increase the microhardness of the nanocrystalline nickel matrix. There have been a large number of publications on the synthesis and properties of N-TiO_2 electrodeposited composite coatings[39-45]. It was found that Ni-TiO_2 coatings having anatase particles exhibited higher microhardness and improved wear resistance [39-46].

Among the other important metal oxides, cerium oxide/ceria (CeO_2) is widely used as a gas sensor, electrode material for solid oxide fuel cells, oxygen pumps, amperometric oxygen monitors, and catalytic supports for automobile exhaust system and as an abrasive for Chemical Mechanical Polishing (CMP) slurry. Ceria has also been explored as an important distributive phase for Ni-electrodeposited coatings to improve the corrosion resistance properties[47-50]. The synergistic effect makes CeO_2–TiO_2 composites attractive for a wide range of applications as shown in Figure 1 ranging from photocatalysis to industrial coatings and these applications highlight the versatility and importance of ceria-titania powders in various sectors[51]. However, there are no reports on the Ni-composite coatings containing both ceria and titania particles.

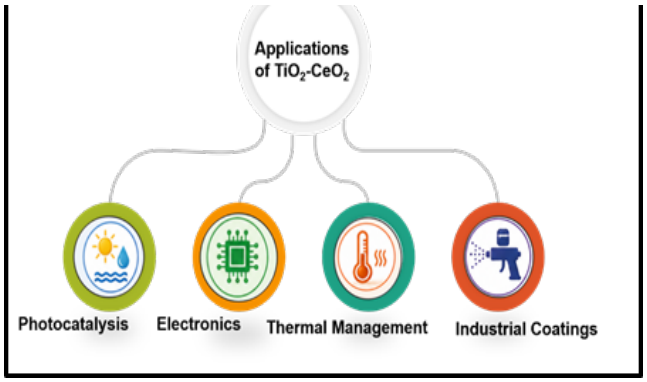


Figure 1. Schematic showing the applications of TiO_2-CeO_2 powder.

In the present work, to obtain the synergistic properties of both titania and ceria in the electrodeposited nickel matrix, a composite powder of titania-ceria is used as the dispersing phase. The effect of applied current density on the corrosion resistance of the coatings was also studied. Furthermore, the powder is prepared using the versatile, cost-effective Solution Combustion Synthesis (SCS)[52-55].

2. Experimental

2.1 Synthesis and Characterization of Titania-Ceria Nanoparticles

The chemicals used for preparation of ceria-titania composite particles are as follows: titania (SD fine Chem Ltd.), ceric ammonium nitrate (SD fine Chem Ltd.), glycine (Merck), urea (merck), hexamine (Loba Chemie) and oxalyl dihydrazide (Loba Chemie). The required composite powder was prepared by solution combustion method using mixture of fuels approach[56-58]. In the present study, 10 g titania powder was dispersed well in water, to which an aqueous mixture of 11.64 g of ceric ammonium nitrate, 1.044 g glycine, 0.094 g urea, 0.1772 g hexamine and 0.1121 g oxalyl dihydrazide was added and stirred well. The redox mixture was then placed in a preheated muffle furnace (400°C). The solution boiled, underwent frothing and ignited to give a uniformly ceria coated titania particles which were light yellow in color. The powder composition corresponds to 73.3 wt% TiO_2 and 26.7 wt% CeO_2 and hereinafter it is referred to as TC powder. The ceria coated titania particles were used for the development of Ni-TC composite coatings. Mixture of fuels were used to reduce the

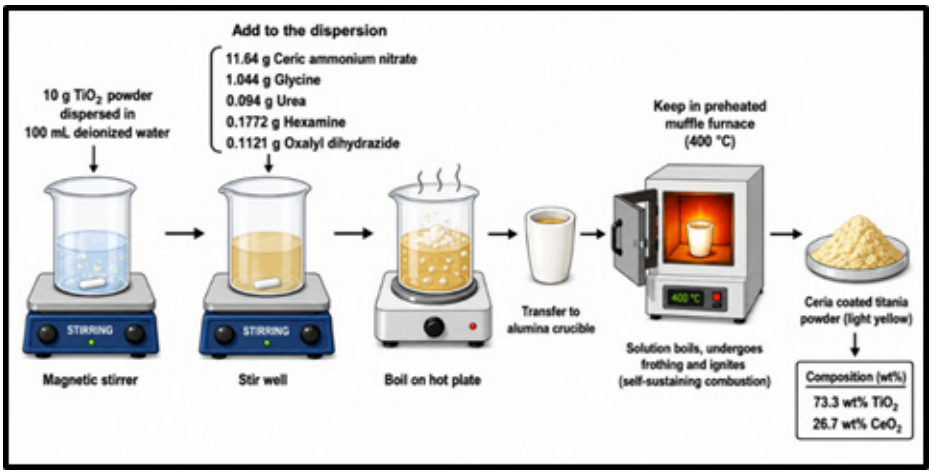


Figure 2. Schematic showing the steps involved in the solution combustion synthesis of TC powder.

exothermicity of the combustion reaction so that the anatase form of titania is retained. Figure 2 shows the schematic depicting the steps involved in SCS of TC powder. "A powder X-ray diffractometer (Bruker, D-8 Advance) was used to identify the phases present in the powder and to calculate the crystallite sizes of the powders from the pattern"[30,50]. "The morphology of the powders and coating microstructure were recorded using Field Emission Scanning Electron Microscope (FESEM, model Carl Zeiss Supra 40 equipped with an Energy-Dispersive X-ray Spectroscope (EDS, Oxford Instruments)[30,50]. The X-ray mapping images and Energy Dispersive X-ray Analysis (EDAX) data was also generated for Ni-TC coating. "Particle size distribution of the powder was obtained using particle size analyzer (Master sizer 2000, Malvern) based on laser diffraction"[30,50].

2.2 Preparation of Ni-TiO_2-CeO_2 (Ni-TC) Composite Coatings and their Characterizations

"A nickel sulfamate bath with the following composition was used: 300 g/L of nickel sulfamate solution (50 g/L of Ni), 10 g/L of nickel chloride, 30 g/L boric acid and 0.2 g/L of sodium lauryl sulfate"[50]. The particle loadings in the bath were 25 g/L and 100 g/L. The bath was stirred overnight at 300 rpm on a magnetic stirrer. The pH of the bath was maintained at 4 by using sulfamic acid and 10% NaOH. "The electrodeposition was carried out using Aplab 7253 regulated DC power supply at various current densities and durations: 0.75A/dm^2 for 6 h, 1.54 A/dm^2 for 3 h, 3.1 A/dm^2 for 1.5 h and 4.65 A/dm^2 for 52 min, on polished and cleaned brass plates for microhardness testing such that the deposit thickness was ~40 µm based on Faraday's laws[50]". Figure 3 shows the schematic of the electrodeposition setup used for developing the coatings. Mild steel substrates were also coated at the same current densities for corrosion tests. Brass pins were also coated for wear tests[30,50]. During electrodeposition the solution was stirred at 400 rpm.

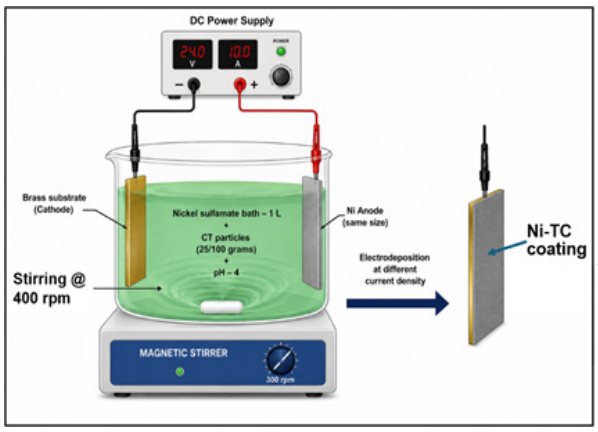


Figure 3. Schematic showing the setup used for carrying out the electrodeposition of Ni-TC composite coatings.

Plain Ni was also electrodeposited at 1.54 A/dm^2 for 3 h on brass substrates.

"The metallographic specimens for cross-sectional studies were prepared by sandwiching electrodeposited Ni-TC coatings followed by mechanical grinding and polishing with Al_2O_3 slurry, down to 0.05 µm. The microhardness measurements were performed at five different locations on the cross-section of each coating (Micromet 2103, Buehler, 50 gF load). The optical micrographs of the coatings cross section were recorded using a vertical metallurgical microscope. The area fraction of particles incorporated in the Ni matrix was calculated from the cross-sectional optical micrographs using image analysis software (Videopro 32 supplied by M/s Leading Edge, Australia)[50]".

"Corrosion behavior of Ni and Ni-TC composite coatings electrodeposited at different current densities on mild steel coupons were conducted using CHI 604 2D electrochemical workstation[30,50]. To eliminate the influence of the coating thickness on the electrochemical measurement parameters, the thickness of the coatings was maintained at 11±1 µm. The test was carried out in deaerated 3.5 wt% (0.6 M) NaCl solution (200±2 ml) using conventional three electrode cell equipped with coated mild steel coupons with an active area of 1cm^2 as working electrode. Platinum foil and Saturated Calomel Electrode (SCE) were used as counter and reference electrodes respectively. The reference electrode was connected to a Luggin capillary, and its tip was placed very close to the surface of the working electrode to minimize IR drop. The coupon was immersed in NaCl solution for an hour in order to establish the Open Circuit Potential (E_{OCP}). The system was allowed to attain open circuit potential then the upper and lower potential limits of linear sweep voltammetry were set at ±200 mV with respect to the E_{OCP}. The sweep rate was 1 mV/s. The Tafel plots obtained have been represented as potential vs. log i plot".

The corrosion potential (E_{corr}), corrosion current density (i_{corr}) and polarization resistance (Rp) were deduced from the Tafel plot. The polarization resistance was obtained using the Stern–Geary equation using the i_{corr} and Tafel constants.

The equation is:

$$i_{corr} = \frac{B}{R_p} \qquad \text{Equation (1)}$$

The Stern–Geary constant is given by:

$$B = \frac{\beta_a \beta_c}{2.303(\beta_a + \beta_c)} \qquad \text{Equation (2)}$$

Where β_a and β_c are Tafel slopes or the Tafel constants, expressed in mV/dec.

Corrosion Rates (CR) were calculated by the following equation:

$$CR = \frac{1.13\, i_{corr} X\ Eq.\ wt\ .of\ Ni}{Density\ of\ Ni} \qquad \text{Equation (3)}$$

Wear tests were done on a pin-on-disc tribometer to understand the tribological behavior of composite coatings. The details are already discussed in our previous publications[35, 50].

3. Results and Discussions

3.1 Characterization of Powders

The FESEM images of titania-ceria particles showed near to spherical particles with particle size in the range of 50-150 nm (Figure 4(a) and (b)). Even though the particles were in nanosize (from FESEM), the Titania-Cerium oxide (TC) particles were agglomerated to a larger extent with an average agglomerated particle size of 2.753 µm as obtained by particle size analysis. The bimodal distribution seen in the particle size analysis clearly indicates the presence of two different ranges of agglomerates of particles.

Figure 5 shows the particle size distribution curves of commercial titania and SCS synthesized TC powders. The particle size analysis of commercial titania showed a d(0.1), d(0.5) and d(0.9) of 0.733, 1.705 and 11.055 µm. The particle size analysis of TC powder showed a d(0.1), d(0.5) and d(0.9) of 0.830, 2.753 and 40.119 µm respectively. The bimodal distribution clearly shows the presence of fine peak corresponding to individual particles/small agglomerates, and the second peak corresponding to larger agglomerates.

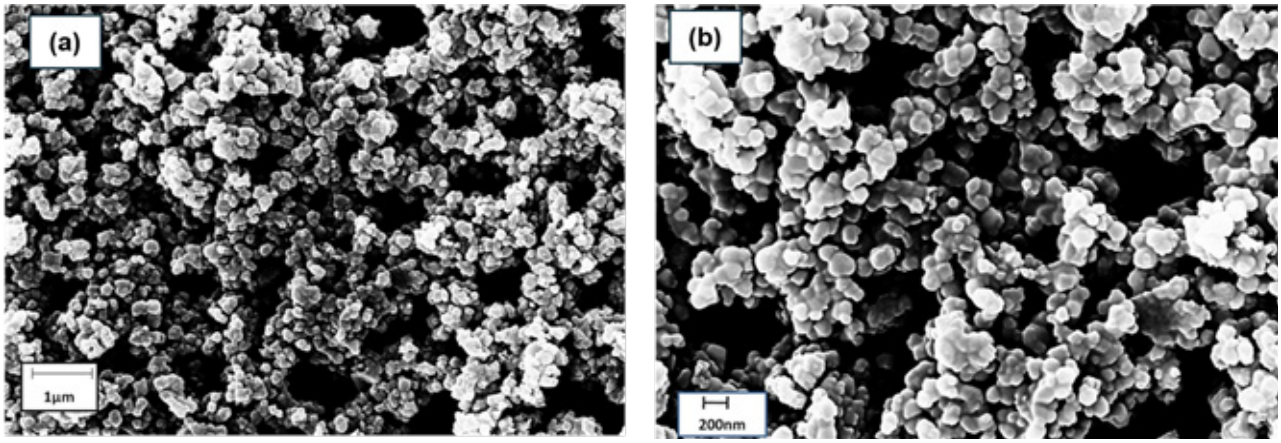


Figure 4. FESEM images of TC powder in two different magnifications.

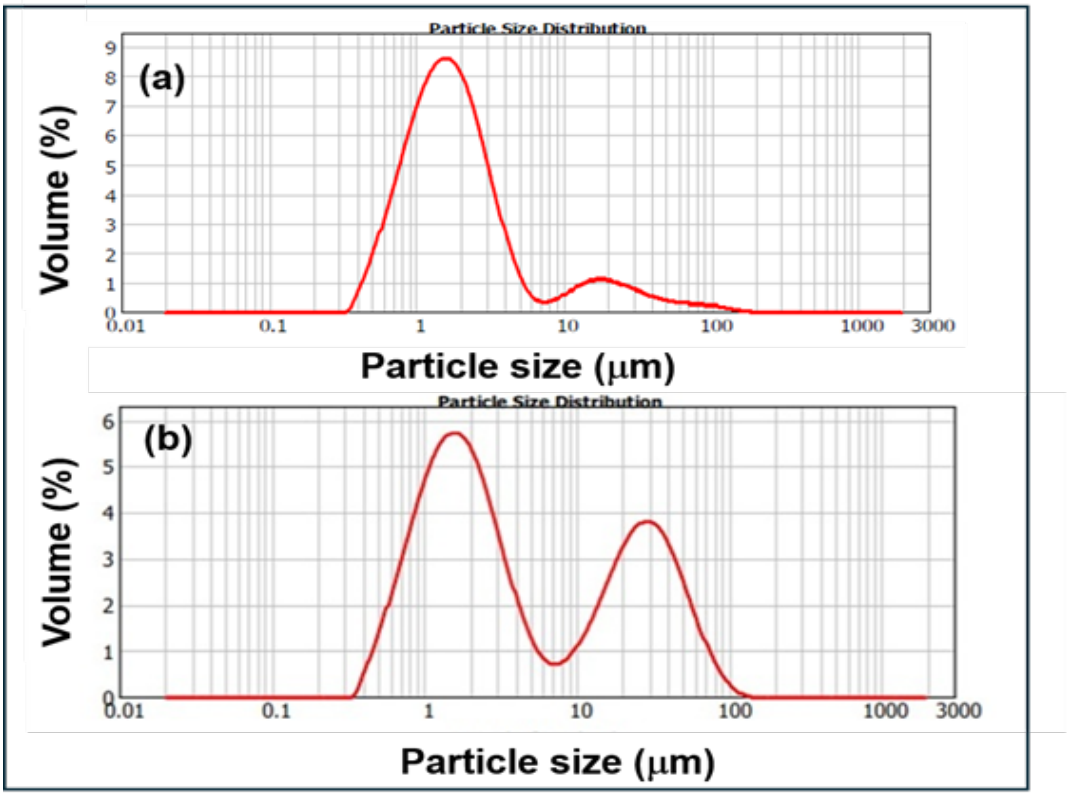


Figure 5. Particle size distribution curves of **(a)** commercial TiO_2 and **(b)** SCS synthesized titania-cerium oxide powder.

Figure 6 shows the powder XRD pattern of TC powder. The XRD pattern shows the presence of anatase titania (JCPDS Card no. 21-1272) as the major phase. The peaks corresponding to cubic fluorite structure of cerium oxide (JCPDS Card no. 34-0394) are also observed.

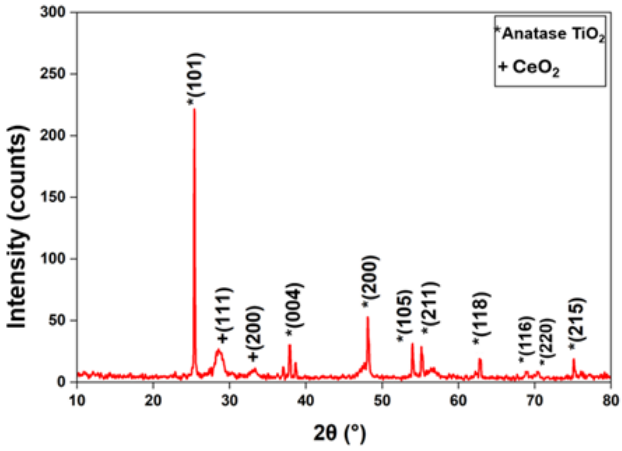


Figure 6. X-ray diffraction showing the characteristic peaks of titania and ceria powders.

3.2 Characterization of Coatings

The cross-sectional images of titania-cerium oxide composite coatings for two different concentrations at varying current densities are shown in Figures 7 and 8. Figure 7 shows the optical micrographs of composite coatings corresponding to lower concentration of particles (25 g/L) while Figure 8 shows the optical micrographs of composite coatings for higher concentrations of particles (100 g/L). From the figures, it is inferred that lower current densities and higher concentration of particles yield Ni-CT composite coatings with higher particle incorporation, which is beneficial for improving the microhardness and other properties of the coating. The mechanism of particle incorporation in electrodeposited Ni-composite

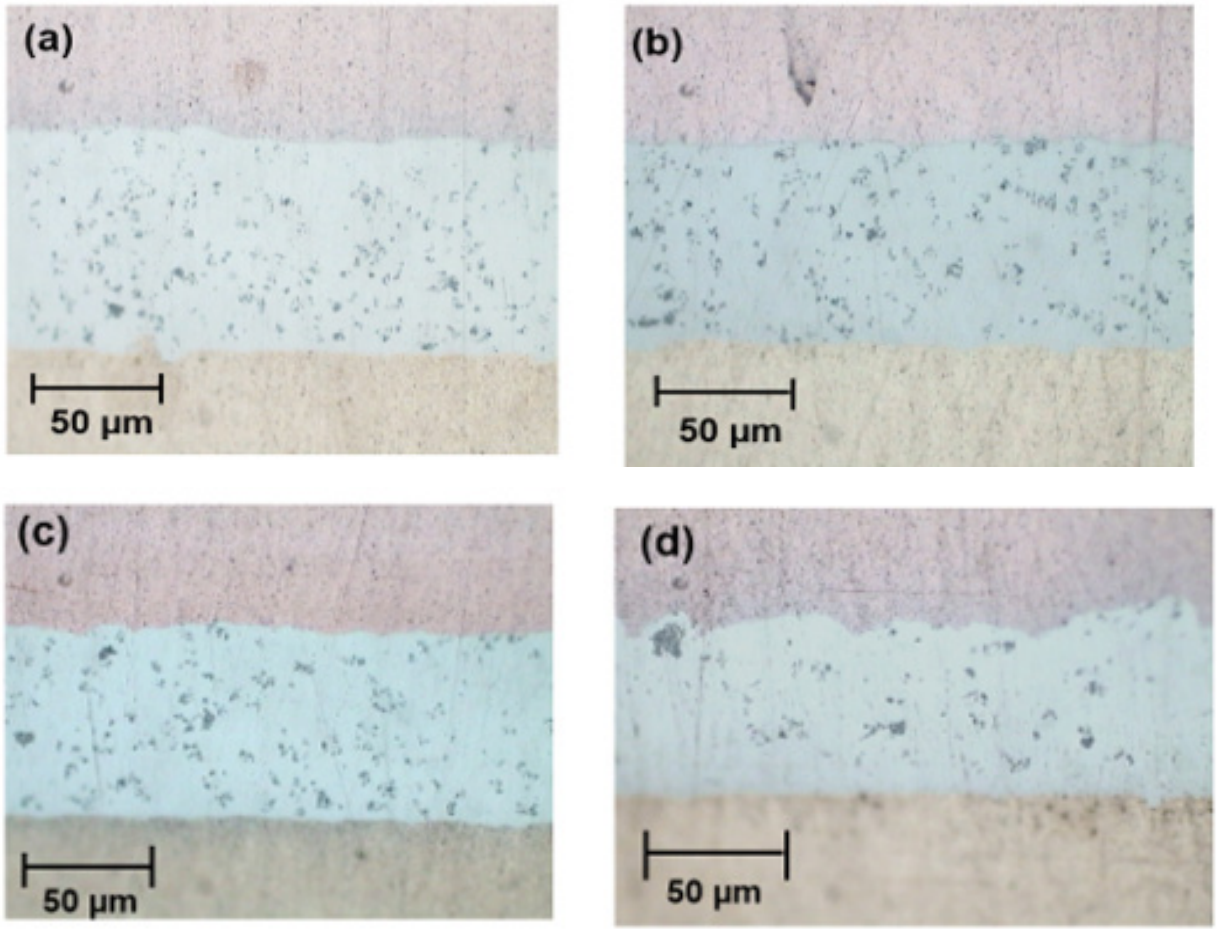


Figure 7. Effect of different current densities on the incorporation of TC particles in the Nickel-TC composite coatings electrodeposited from 25 g/L bath at **(a)** 0.75 A/dm^2, **(b)** 1.54 A/dm^2, **(c)** 3.1 A/dm^2 and **(d)** 4.65 A/dm^2.

coatings has been well explained by Guglielmi model[59]. As per this mechanism, in the first step, particles are loosely adsorbed onto the cathode through van der Waals forces. In the next step, under sufficient cathodic overpotential, the particles are well adhered to the cathode and are engulfed by the growing nickel deposit[59].

From the plots (Figure 9) it is apparent that irrespective of the current density higher microhardness values were obtained for the coatings electrodeposited from a higher particle content bath and also higher microhardness values were obtained for the coatings electrodeposited at lower current density. Higher the number of particles incorporated in the Ni matrix, higher will be the microhardness[60,61]. With increasing current density, the Ni deposition rate increases. At lower current densities, since the Ni electrodeposition is relatively slow, the particles in the bath find sufficient time to adsorb onto the cathode and easily get incorporated in the growing nickel layer. On the other hand, at higher current densities, due to the vigorous evolution of H_2 gas, loosely adsorbed particles are knocked out by the H_2 gas, thereby reducing the particle incorporation into the nickel matrix. The uniform distribution of TC particles within the Ni matrix impacts the microhardness and other properties. The microhardness values of the Ni-TC composite coatings are higher than that of electrodeposited plain nickel which is ~ 300 HK. The particles serve as physical barriers that inhibit the growth of nickel grains and reduce the plastic deformation under various loads. This results in grain refinement and dispersive strengthening effect, thereby in turn increasing the microhardness and wear resistance of the Ni-TC composite coatings. The area fraction of particles was calculated using the J-image software. The area fraction of particles incorporated were 8.1, 7.2, 6.8 and 6.0 % respectively at current densities of 0.75A/dm^2 for 6 h, 1.54 A/dm^2 for 3 h, 3.1 A/dm^2 for 1.5 h and 4.65 A/dm^2 for 52 min.

The surface FESEM image of the Ni-TC coating electrodeposited from 100 g/L bath at 1.54A/dm^2 is

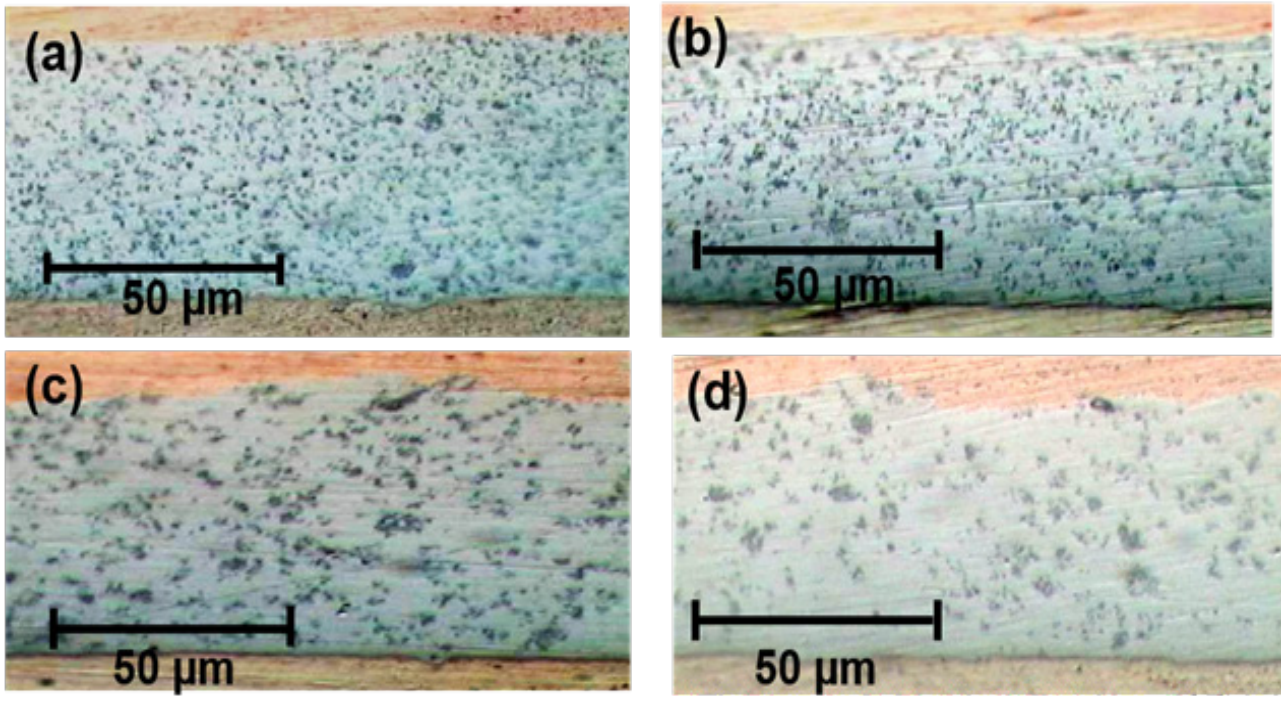


Figure 8. Effect of different current densities on the incorporation of TC particles in the Nickel-TC composite coatings electrodeposited from 100 g/L bath at **(a)** 0.75 A/dm^2, **(b)** 1.54 A/dm^2, **(c)** 3.1 A/dm^2 and **(d)** 4.65 A/dm^2.

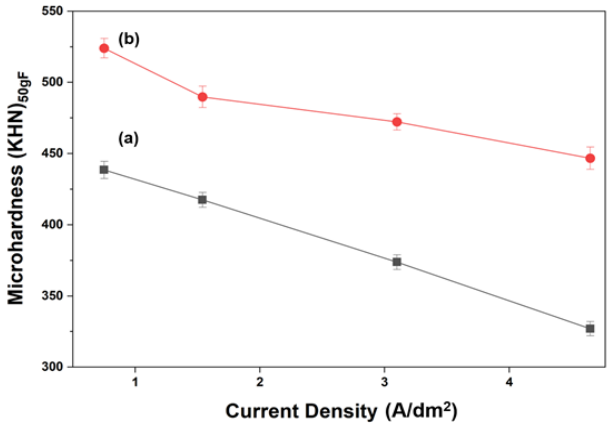


Figure 9. Microhardness vs current density plots of Ni-TC composite coatings electrodeposited from the nickel sulfamate bath containing **(a)** 25 and **(b)** 100 g/L of CT particles.

shown in Figure 10. The Ni grains are seen along with codeposited TC particles. Figure 11 (a) shows the X-ray mapping images of the Ni-TC coating. It clearly shows the uniform distribution of particles as evident from the image of Ti element. The EDAX spectral data (Figure 11(b)) of the surface FESEM clearly shows ~7.5 wt% of particles in the Ni matrix.

The XRD pattern of the Ni-TC composite coating electrodeposited at 1.54 A/dm^2 from 100 g/L bath is shown in Figure 12. The XRD peaks correspond to metallic nickel (JCPDS card no. 004-0850) and anatase TiO_2 (JCPDS Card no. 21-1272). Peaks corresponding

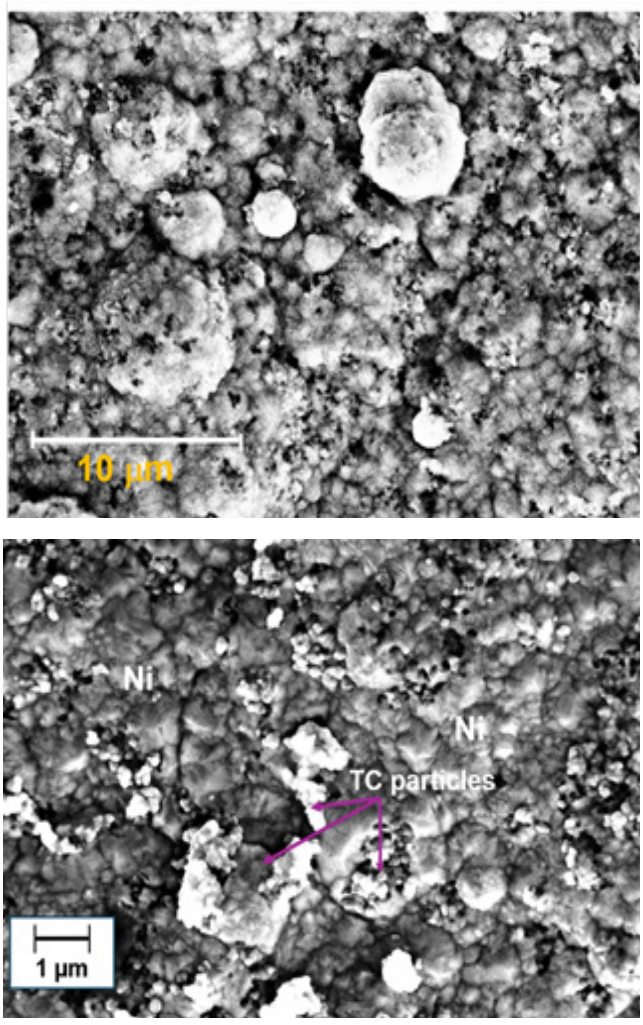


Figure 10. FESEM images of Ni-TC coatings at different magnifications.

Table 1. Corrosion potential, corrosion rates and Tafel slopes calculated from potentiodynamic plots for Ni-TC composite coatings (100 g/L)

Current density A/dm²	E_{corr} (V)	i_{corr} (A/cm²)	βa (mV/dec)	βc (mV/dec)	Rp Ωcm²
0.75	−0.388	1.22×10^{-8}	236.5	137.8	3.10×10^{6}
1.54	−0.291	2.04×10^{-7}	204.8	121.2	1.62×10^{5}
3.10	−0.322	3.27×10^{-7}	250.9	112.3	1.03×10^{5}
4.65	−0.319	6.55×10^{-7}	265.4	143.0	6.16×10^{4}

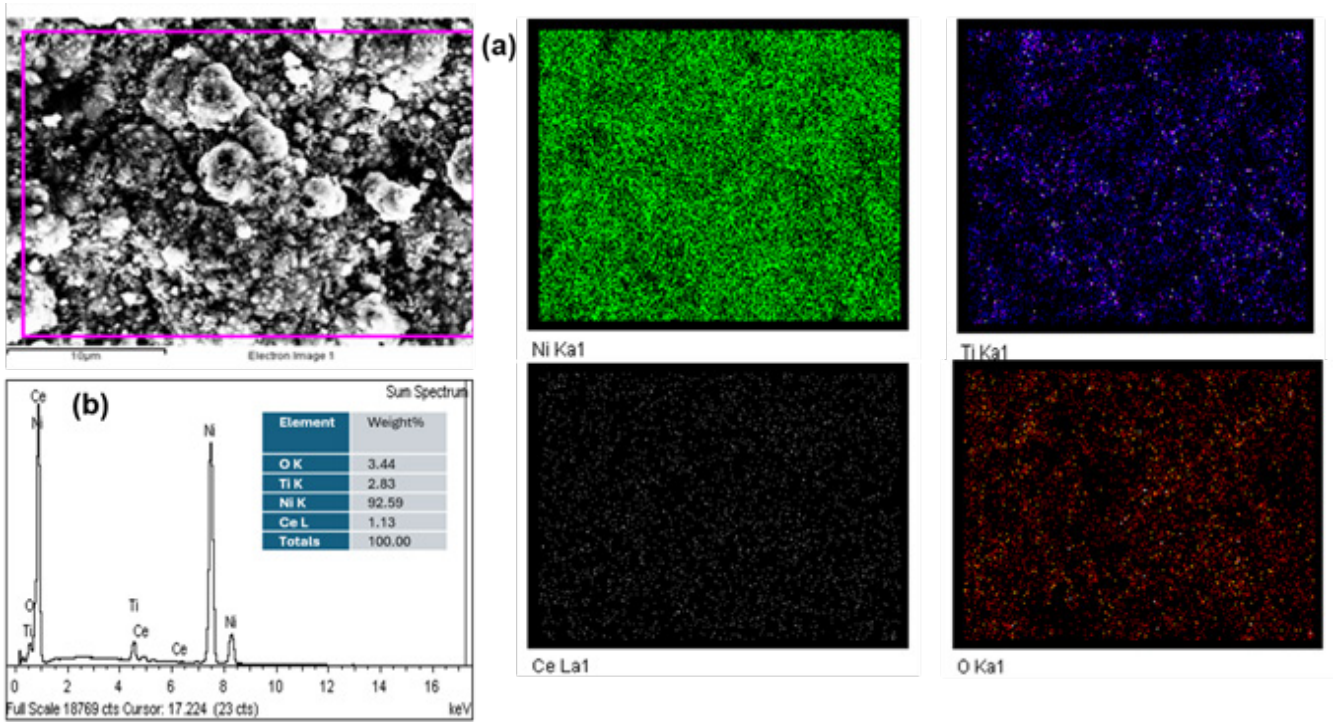


Figure 11. (**a**) X-ray mapping images corresponding to the elements Ni, Ti, Ce and O and (**b**) EDAX data and spectrum of Ni-TC coating.

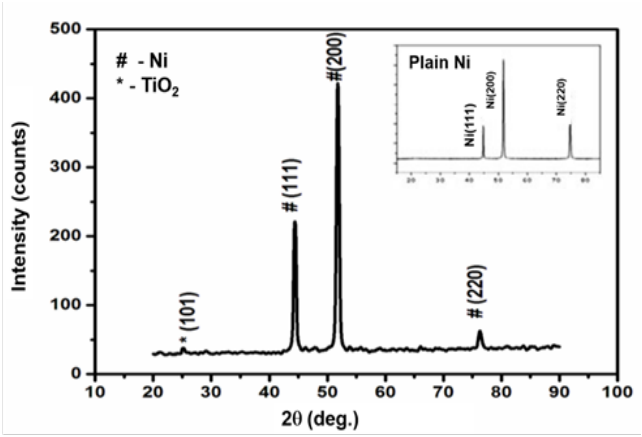


Figure 12. XRD of Ni-TC composite coating electrodeposited at 1.54 A/dm^2 (100 g/L).

to ceria are not observed due to the lower ceria content in the TC powder.

The corrosion potential, the corrosion current, and the polarization resistance obtained from the Tafel plots are listed in Table 1. The kinetics of the corrosion reaction is obtained from corrosion current density (I_{corr}) and I_{corr} is inversely proportional to the corrosion current density. With increasing TC particle incorporation into the nickel matrix, the corrosion resistance increases due to the grain refinement. Improved corrosion resistance is attributed to the reinforcement of uniformly dispersed TC particles in the Ni matrix followed by synergistic effect of dispersion strengthening and microstructure modification[60].

Figures 13 shows the Tafel plots of Ni-TC coating electrodeposited from 100 g/L bath at different current densities. At lower current densities where the particle incorporation is more, the corrosion potential is more positive, and the corrosion current is low which suggests an increase in corrosion resistance. The obtained corrosion results are complimented by the potentiodynamic polarization resistance values.

Table 2. Comparison of microhardness, Icorr and Rp values of Ni-TC coating of the present study vis-à-vis Ni-TiO_2, Ni-CeO_2 and Ni-Al_2O_3 coatings

Coating	Knoop microhardness @50 gF	i_{corr} (μA/cm²)	Rp (Ω cm²)	Reference
Ni	300	0.6267	4820	[36]
Ni-TiO_2 (commercial)	520	0.3900	86620	[46]
Ni-CeO_2	508	0.3660	40520	[50]
Ni-Al_2O_3	550	0.0119	131500	[33]
Ni- 90 wt% Al_2O_3 and 10 wt% cubic zirconia	520	0.3782	31990	[35]
Ni-Yttria doped ceria	480	0.1600	118000	[36]
Ni-TiO_2-CeO_2 (TC)	520	0.0122	3100000	Present study

Table 2 summarizes the microhardness, i_{corr} and Rp values of coatings of the present study vis-à-vis coatings like Ni-TiO_2, Ni-CeO_2, Ni-Al_2O_3, etc. The Ni-TC coating exhibited similar microhardness value of Ni-TiO_2 and improved microhardness over Ni-CeO_2 coating. Further, Ni-TiO_2 has shown 18 times better Rp value compared to plain Ni and Ni-CeO_2 has shown 8.4 times better Rp value compared to plain Ni. It is interesting to note that Ni-TC coating has shown 643 times better Rp values compared to plain Ni, Ni-CeO_2 and Ni-TiO_2. This may be attributed to the grain refinement and incorporation of uniform sized TC particles in the Ni matrix.

A decrease of I_{corr}, i.e., corrosion current density in the presence of particles has been observed. This indicates a more efficient protective action of Ni-composite coatings compared to pure Ni-coatings as reported in literature. The anodic and cathodic slopes

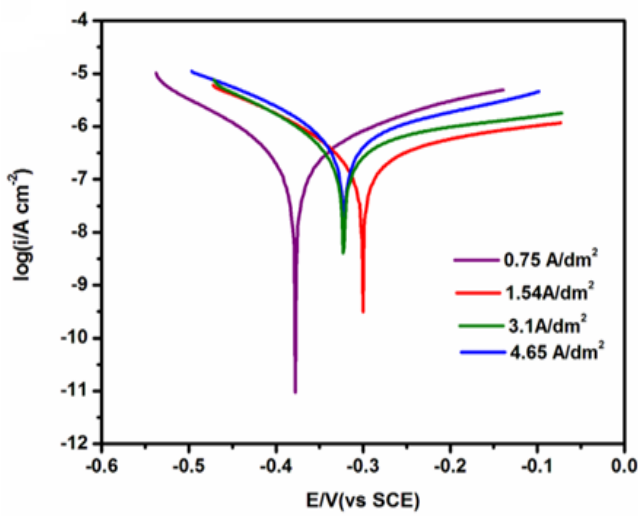


Figure 13. Tafel plots of Ni-TC coatings electrodeposited from 100 g/L bath at different current densities.

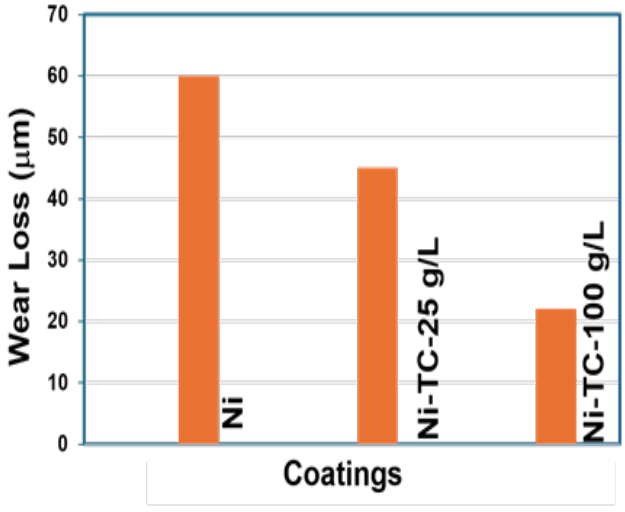


Figure 14. A histogram showing the wear loss for different composite coatings.

(βa and βc) are also slightly modified by the presence of particles. This behavior can be ascribed to the surface blockage by the oxide. Thus, the anodic dissolution and cathodic hydrogen evolution reactions were inhibited by particles through the blockage of the reaction sites in the mild steel surface without affecting the anodic and cathodic mechanisms. The composite coating exhibits a higher polarization resistance compared to plain Ni and undergoes uniform corrosion. Unlike plain nickel coating that undergoes pitting corrosion, the Ni-composite coating undergoes uniform corrosion[50]. The compact nature of the coatings obstructs the entry of Cl^- ions entering from solution to the electrode surface.

Electrodeposited Ni-TC composite coatings were tested on a pin-on-disc tribometer. The tests were done on a track radius of 30 mm at room temperature in an environment of relative humidity 45 for a load of 1kgf. The Ni-TC coating exhibited lower wear loss compared to plain Ni (Figure 14).

In the present study, CT particles corresponding to 73 wt% TiO_2 and 27 wt% CeO_2 were used. The interesting results realized in this study open up new research possibilities. A detailed study by systematically varying the ceria and titania content in the TC compositions will be attempted in the future work.

4. Conclusions

Titania-Ceria composite powders are propitious distributive phase for electrodeposited composite coatings. In the present study, TC particles corresponding to 73 wt% TiO_2 and 27 wt% CeO_2 were synthesized using mixture of fuels approach and the particles were <200 nm in size and showed bimodal distribution. Higher particle loaded bath (100 g/L) facilitated the formation of Ni-composite coatings with more particle incorporation. The lower current density facilitated higher particle incorporation in the Ni matrix and coatings exhibited higher microhardness values. The coating with large number of particles (100 g/L) electrodeposited at lower current density exhibited improved corrosion resistance compared to the coatings electrodeposited at higher current densities. Furthermore, the Ni-TC coating exhibited better corrosion resistance compared to Ni-CeO_2 and Ni-TiO_2 coatings.

5. Acknowledgements

The authors thank Mr. VK William Grips for the encouragement and Director CSIR-NAL for the encouragement. The authors thank Mr. G. Srinivas, Mr. Siju and Mr. Muni Prakash for the XRD, FESEM and wear studies.

6. References

1 Low CT, Walsh FC. Electrodeposition of nanostructured materials. 2nd ed. Chichester: Wiley; 2009.

2. Schlesinger M, Paunovic M, editors. Modern Electroplating. 5th ed. Hoboken (NJ): John Wiley & Sons; 2010. https://doi.org/10.1002/9780470602638

3. Paunovic M, Schlesinger M. Electrodeposition: The materials science of coatings and substrates. 2nd ed. New York: Wiley; 2006.

4. Benea L, Bonora PL, Borello A, Martelli S. Electrodeposition of composite coatings. J Appl Electrochem. 2001; 31(5):499-505.

5. Hovestad A, Janssen LJJ. Electrochemical codeposition of inert particles in a metallic matrix. J Appl Electrochem. 1995; 25(6):519-27. https://doi.org/10.1007/BF00573209

6. Safavi MS, Walsh FC. The electrodeposition of particle-metal matrix composite coatings to meet tribological and corrosion challenges. Adv Colloid Interface Sci. 2025;343:103584. https://doi.org/10.1016/j.cis.2025.103584.

7. Vaezi MR, Sadrnezhaad SK, Nikzad L. Electrodeposition of Ni-SiC nanocomposite coatings and evaluation of wear and corrosion resistance and electroplating characteristics. Colloids Surf A Physicochem Eng Asp. 2008; 315(1-3):176-182. https://doi.org/10.1016/j.colsurfa.2007.07.027

8. Srivastava M, Selvi VE, Grips VKW, Rajam KS. Influence of SiC, Si_3N_4 and Al_2O_3 particles on the structure and properties of electrodeposited Ni-based composite coatings. Mater Lett. 2008; 62(21-22):3487-3489. https://doi.org/10.1016/j.matlet.2008.03.008

9. Thiemig D, Bund A. Characterization of electro-deposited Ni-SiC nanocomposite coatings. Surf Coat Technol. 2009; 203(20-21):2976-2985.
10. Gyawali G, Joshi B, Lee SW. Corrosion and wear behavior of electrodeposited Ni-Al_2O_3 nanocomposite coatings. Appl Surf Sci. 2011; 257(12):5204-5210.
11. Low CTJ, Wills RGA, Walsh FC. Electrodeposition of composite coatings containing nanoparticles in a metal deposit. Surf Coat Technol. 2006; 201(1-2):371-383. https://doi.org/10.1016/j.surfcoat.2005.11.123
12. Walsh FC, Wang S, Zhou N. The electrodeposition of composite coatings: Diversity, applications and challenges. Curr Opin Electrochem. 2020; 20:8-19. https://doi.org/10.1016/j.coelec.2020.01.011
13. Lelevic A, Walsh FC. Electrodeposition of Ni-P composite coatings: A review. Surf Coat Technol. 2019; 378:124803. https://doi.org/10.1016/j.surfcoat.2019.07.027
14. Sajjadnejad M, Haghshenas SMS, Badr P, Setoudeh N, Hosseinpour S. Wear and tribological characterization of nickel matrix electrodeposited composites: A review. Wear. 2021; 486-487:204098. https://doi.org/10.1016/j.wear.2021.204098
15. Mahidashti Z, Aliofkhazraei M, Lotfi B. Review of nickel-based electrodeposited tribo-coatings. Trans Indian Inst Met. 2018; 71(2):257-295. https://doi.org/10.1007/s12666-017-1175-x
16. Baghery P, Farzam M, Mousavi AB, Hosseini M. Ni-TiO_2 nanocomposite coating with improved wear and corrosion resistance deposited by pulse electrodeposition. Surf Coat Technol. 2010; 204(23):3804-3810. https://doi.org/10.1016/j.surfcoat.2010.04.061
17. Wang C, Shen Y, Wang H. Characterization of Ni-CeO_2 nanocomposite coatings prepared by jet electrodeposition and their corrosion resistance. J Alloys Compd. 2017; 727:269-278. https://doi.org/10.1016/j.jallcom.2017.08.105
18. Chen XH, Chen CS, Xiao HN, Cheng FQ, Zhang G, Yi GJ. Corrosion behavior of carbon nanotube-nickel composite coatings prepared by electrodeposition. Surf Coat Technol. 2005; 191(2-3):351-356. https://doi.org/10.1016/j.surfcoat.2004.04.055
19. Hou KH, Sheu HH, Ger MD, Wang LM. Preparation and properties of Ni-Al_2O_3 nanocomposite coatings by pulse electrodeposition. Appl Surf Sci. 2008; 254(20):6887-6893.
20. Ramesh S, Raghavendra CR, Aliofkhazraei M. Electrodeposition of Ni-based nanocomposite coatings: A comprehensive review. Inorg Nano-Met Chem. 2018; 48(1):1-17. https://doi.org/10.1080/24701556.2019.1567537
21. Oluwasegun KM, *et al.* A review on properties of electrodeposited nickel composite coatings: Ni-Al_2O_3, Ni-SiC, Ni-ZrO_2, Ni-TiO_2 and Ni-WC. Materials (Basel). 2024; 17:5715. https://doi.org/10.3390/ma17235715 PMid:39685150 PMCid:PMC11642598.
22. Guan T, Zhang N. Recent advances in electrodeposition of nickel-based nanocomposites enhanced with lubricating nanoparticles. Nanomanuf Metrol. 2024; 7:25. https://doi.org/10.1007/s41871-024-00245-6 PMid:39679139 PMCid:PMC11638300.
23. Aruna ST. Studies on electrodeposited Ni-composite coatings containing cost-effective and exemplary distributed phases. J Electrochem Soc India. 2021; 70(3-4):67-75.
24. Aruna ST, Latha S, Lakshmi RV. Multifunctional properties of electrodeposited nickel composite coating containing nanosized monoclinic zirconia particles. J Metall Mater Sci. 2020; 62:77-91.
25. Aruna ST, Arunima S, Latha S, William Grips VK. Preparation of oil encapsulated microcapsules and tribological property of Ni composite coating containing them. Mater Manuf Process. 2016; 31:107-111. https://doi.org/10.1080/10426914.2014.973585
26. Aruna ST, Lakshmi PG, Seema HM. The effect of additives on the properties of electrodeposited Ni-zircon composite coatings. RSC Adv. 2016; 6:11185-11192. https://doi.org/10.1039/C5RA25119B
27. Aruna ST, Srinivas G. Wear and corrosion resistant properties of electrodeposited Ni composite coating containing Al_2O_3-TiO_2 composite powder. Surf Eng. 2015; 31(9):708-713. https://doi.org/10.1179/1743294415Y.0000000050
28. Aruna ST, Anandan C, William Grips VK. Effect of probe sonication and sodium hexametaphosphate on the microhardness and wear behavior of electrodeposited Ni-SiC composite coating. Appl Surf Sci. 2014; 301:383-390. https://doi.org/10.1016/j.apsusc.2014.02.087
29. Aruna ST, Roy S, Sharma A, Savitha G, William Grips VK. Cost-effective wear and oxidation resistant electrodeposited Ni-pumice coating. Surf Coat Technol. 2014; 251:201-209. https://doi.org/10.1016/j.surfcoat.2014.04.026

30. Aruna ST, Savitha G, Shedthi J, William Grips VK. The corrosion resistance of nickel electrocomposite coating containing $BaFe_{12}O_{19}$ particles. ISRN Corros. 2013; 2013:192684. https://doi.org/10.1155/2013/192684

31. Aruna ST, William Grips VK. Electrodeposited nickel composite coating containing in-situ nickel impregnated alumina particles. Mater Lett. 2012; 66:141-144. https://doi.org/10.1016/j.matlet.2011.08.065

32. Aruna ST, Srikanth PVK, Ahamad MJ, Latha S, Rajam KS. Optimization of the properties of electrodeposited Ni-YSZ composites using Taguchi method and regression analysis. Port Electrochim Acta. 2011; 29:23-36. https://doi.org/10.4152/pea.201101023

33. Aruna ST, EzhilSelvi V, William Grips VK, Rajam KS. Corrosion and wear resistant properties of Ni-Al_2O_3 composite coatings containing various forms of alumina. J Appl Electrochem. 2011; 41:461-471. https://doi.org/10.1007/s10800-011-0256-5

34. Aruna ST, William Grips VK, Rajam KS. Synthesis and characterization of Ni-Al_2O_3 composite coatings containing different forms of alumina. J Appl Electrochem. 2010; 40:2161-2169. https://doi.org/10.1007/s10800-010-0198-3

35. Aruna ST, William Grips VK, Rajam KS. Ni-based electrodeposited composite coating exhibiting improved microhardness, corrosion and wear resistance properties. J Alloys Compd. 2009; 468:546-552. https://doi.org/10.1016/j.jallcom.2008.01.058

36. Aruna ST, William Grips VK, EzhilSelvi V, Rajam KS. Synthesis and properties of electrodeposited nickel/yttria doped ceria nanocomposite coatings. J Appl Electrochem. 2007; 37:991-1000. https://doi.org/10.1007/s10800-007-9338-9

37. Aruna ST, Diwakar S, Jain A, Rajam KS. Comparative study on the effect of current density on Ni and Ni-Al_2O_3 nanocomposite coatings produced by electrolytic deposition. Surf Eng. 2005; 21(5):209-214. https://doi.org/10.1179/174329405X50037

38. Qiu H, Wang D, Yin S. The microstructure, wear and electrochemical properties of electrodeposited Ni-diamond composite coatings: Effect of diamond concentration. Mater Today Commun. 2023; 34:105476. https://doi.org/10.1016/j.mtcomm.2023.105476

39. Aruna ST, Rajam KS. Synthesis, characterisation and properties of Ni/PSZ and Ni/YSZ nanocomposites. Scr Mater. 2003; 48:507-512. https://doi.org/10.1016/S1359-6462(02)00498-0

40. Li J, Sun Y, Sun X, Qiao J. Mechanical and corrosion-resistance performance of electrodeposited titania- nickel nanocomposite coatings. Surf Coat Technol. 2005; 192:331-5. https://doi.org/10.1016/j.surfcoat.2004.04.082

41. Yang XK, Li Q, Hu JY, Zhong XK, Zhang SY. The electrochemical corrosion behavior of sealed Ni-TiO_2 composite coating for sintered NdFeB magnet. J Appl Electrochem. 2010; 40:39-47. https://doi.org/10.1007/s10800-009-9961-8

42. Parida G, Chaira D, Chopkar M, Basu A. Synthesis and characterization of Ni-TiO_2 composite coatings by electro-codeposition. Surf Coat Technol. 2011; 205:4871-9. https://doi.org/10.1016/j.surfcoat.2011.04.102

43. Baghery P, Farzam M, Hosseini M. Ni-TiO_2 nanocomposite coating with high resistance to corrosion and wear. Surf Coat Technol. 2010; 204:3804-10. https://doi.org/10.1016/j.surfcoat.2010.04.061

44. Sun XJ, Li JG. Tribological characterization of electrodeposited nickel-titania nanocomposite coatings sliding against silicon nitride in high vacuum. Surf Eng. 2008; 24:236-9. https://doi.org/10.1179/174329408X286060

45. Sun XJ, Li JG. Friction and wear properties of electrodeposited nickel-titania nanocomposite coatings. Tribol Lett. 2007; 28:223-8. https://doi.org/10.1007/s11249-007-9254-5

46. Aruna ST, MuniPrakash M, William Grips VK. Effect of titania particles preparation on the properties of Ni-TiO_2 electrodeposited composite coatings. J Appl Electrochem. 2013; 43:805-15. https://doi.org/10.1007/s10800-013-0565-y

47. Li J, Xiong D, Huang Z, Kong J, Dai J. Effect of Ag and CeO_2 on friction and wear properties of Ni-Base composite at high temperature. Wear. 2009; 267:576-584, https://doi.org/10.1016/j.wear.2008.12.050

48. Zhang Z, Lu X, Han B, Luo J. Rare earth effect on the microstructure and wear resistance of Ni-Based coatings. Mater Sci Eng, A. 2007; 454-455:194-202. https://doi.org/10.1016/j.msea.2006.11.034

49. Han B, Lu X. Tribological and anti-corrosion properties of Ni-W-CeO_2 coatings against molten glass. Surf Coat Technol. 2008; 202:3251-3256. https://doi.org/10.1016/j.surfcoat.2007.11.031

50. Aruna ST, Bindu CN, Ezhil Selvi V, William Grips VK, Rajam KS. Synthesis and properties of electrodeposited Ni/CeO_2 nanocomposite coatings. Surf Coat Technol.

2006; 200:6871-6880. https://doi.org/10.1016/j.surfcoat.2005.10.035

51. Kadhim F, Baqer A, Shanan Z, Tameem M. Synthesis of TiO_2, CeO_2 and their composite nanostructures for gas sensor applications. AIP Conf Proc. 2021; 2372:180009. https://doi.org/10.1063/5.0065721
52. Aruna ST, Mukasyan AS. Combustion synthesis and nanomaterials. Curr Opin Solid State Mater Sci. 2008; 12:44-50. https://doi.org/10.1016/j.cossms.2008.12.002
53. Patil KC, Aruna ST, Mimani T. Combustion synthesis: an update. Curr Opin Solid State Mater Sci. 2002; 6:507-512. https://doi.org/10.1016/S1359-0286(02)00123-7
54. Patil KC, Aruna ST, Ekambaram S. Combustion synthesis. Curr Opin Solid State Mater Sci. 1997; 2:158-165. https://doi.org/10.1016/S1359-0286(97)80060-5
55. Patil KC, Hegde MS, Rattan T, Aruna ST. Chemistry of nanocrystalline oxide materials: Combustion synthesis, properties and applications. Singapore: World Scientific; 2008. https://doi.org/10.1142/6754
56. Aruna ST, Rajam KS. Mixture of fuels approach for the solution combustion synthesis of Al_2O_3-ZrO_2 nanocomposite. Mater Res Bull. 2004; 39:157-167. https://doi.org/10.1016/j.materresbull.2003.10.005
57. Aruna ST, Kini NS, Rajam KS. Solution combustion synthesis of CeO_2-$CeAlO_3$ nanocomposites by mixture-of-fuels approach. Mater Res Bull. 2009; 44:728-733. https://doi.org/10.1016/j.materresbull.2008.09.034
58. Aruna ST, Kini NS, Shetty S, Rajam KS. Synthesis of nanocrystalline $CeAlO_3$ by solution-combustion route. Mater Chem Phys. 2010; 119(3):485-489. https://doi.org/10.1016/j.matchemphys.2009.10.001
59. Guglielmi N. Kinetics of the deposition of inert particles from electrolytic baths. J Electrochem Soc. 1972; 119(8):1009-1012. https://doi.org/10.1149/1.2404383
60. Benea, L. Electrodeposition and tribocorrosion behaviour of ZrO_2-Ni composite coatings. J Appl Electrochem. 2009; 39:1671-1681. https://doi.org/10.1007/s10800-009-9859-5
61. Zellele DM, Yar-Mukhamedova GS, Rutkowska-Gorczyca M. A review on properties of electrodeposited nickel composite coatings: Ni-Al_2O_3, Ni-SiC, Ni-ZrO_2, Ni-TiO_2 and Ni-WC. Materials. 2024; 17(23):5715. https://doi.org/10.3390/ma17235715 PMid:39685150 PMCid:PMC11642598.

Author Contribution

J. Ann Miriam: Writing –Validation, Investigation, Formal analysis, Data curation. Methodology. N. Balaji: Formal Analysis, Validation, Funding acquisition. S.T. Aruna: Methodology, Project administration, Supervision, Resources, Writing – review & editing. All authors have read and agreed to the published version of the manuscript.